Review of Scientific Instruments

Comb-locked cavity-assisted double-resonance molecular spectroscopy based on diode lasers

Cite as: Rev. Sci. Instrum. **92**, 073003 (2021); https://doi.org/10.1063/5.0054592
Submitted: 20 April 2021 . Accepted: 26 June 2021 . Published Online: 14 July 2021

C.-L. Hu, J. Wang, T.-P. Hua, A.-W. Liu, Y. R. Sun, and S.-M. Hu

Review of Scientific Instruments ARTICLE scitation.org/journal/rsi

Comb-locked cavity-assisted double-resonance molecular spectroscopy based on diode lasers

Cite as: Rev. Sci. Instrum. 92, 073003 (2021); doi: 10.1063/5.0054592
Submitted: 20 April 2021 • Accepted: 26 June 2021 •
Published Online: 14 July 2021

C.-L. Hu,[1] J. Wang,[1,2] T.-P. Hua,[1] A.-W. Liu,[1,2] Y. R. Sun,[1,2] and S.-M. Hu[1,2,a)]

AFFILIATIONS

[1] Hefei National Laboratory for Physical Sciences at Microscale, iChem Center, University of Science and Technology of China, Hefei 230026, China

[2] CAS Center for Excellence in Quantum Information and Quantum Physics, University of Science and Technology of China, Hefei 230026, China

[a)] **Author to whom correspondence should be addressed:** smhu@ustc.edu.cn

ABSTRACT

Interactions between a molecule and two or more laser fields are of great interest in various studies, but weak and highly overlapping transitions hinder precision measurements. We present the method of comb-locked cavity-assisted double resonance spectroscopy based on narrow-linewidth continuous-wave lasers, which allows for state-selective pumping and probing of molecules. By locking two near-infrared diode lasers to one cavity with a finesse at the order of 10^5, we measured all three types of double resonances. Carbon monoxide molecules with selected speeds along the laser beam were excited to vibrationally excited states, and absorption spectra with sub-MHz linewidths were observed. Positions of double resonance transitions were determined with an accuracy of 3.7 kHz, which was verified by comparing to Lamb-dip measurements. The present work paves the way to the pump–probe study of highly excited molecules with unprecedented precision.

I. INTRODUCTION

Rich physics has been explored for atoms and molecules interacting with multi-color optical fields. Atoms interacting with two lasers have been studied for coherent population trapping (CPT),[1] electromagnetically induced transparency (EIT),[2,3] atomic clocks,[4,5] and precision spectroscopy.[6,7] Compared to atoms, molecules have additional internal degrees of freedom of rotations and vibrations, raising more opportunities in the study of interactions with photons. Molecules in two-color laser fields have been studied for state-resolved molecular dynamics,[8] vibration-rotation energy relaxation,[9–13] and population transfer.[14,15] Optical–optical double resonance (OODR) spectroscopy of molecules has been applied to label transitions,[16,17] simplify congested spectra,[13] and probe energy levels that are hardly accessible by single-photon transitions.[18–20] All-optical triple resonance spectroscopy has also been demonstrated.[21]

Vibrational transitions of molecules are relatively weaker than electronic transitions. Consequently, it is more challenging to pump enough molecules to selected vibrationally excited states and probe them with sufficient sensitivity. However, effective pumping and probing are needed in precision spectroscopy of molecules with interests in fundamental physics, such as testing the quantum electrodynamics theory,[22,23] determination of fundamental physical constants,[24,25] and searching the parity-violating energy difference[26] and the variation of fundamental physical constants.[27] Multi-pass cells and optical resonant cavities have been used to increase the effective optical path length and improve the sensitivity to probe weak transitions,[28] but the pumping efficiency is still a bottleneck. Two-photon precision spectroscopy based on narrow-linewidth continuous-wave (cw) lasers has been limited to strong (Einstein coefficient $A \gg 1\ s^{-1}$) ro-vibrational transitions of molecules.[29–33]

We have recently developed the comb-locked cavity-assisted double resonance (COCA-DR) method based on narrow-linewidth lasers, and the method was first applied to probe ladder-type DR spectra of CO_2.[34] By coupling two continuous-wave milliwatt diode lasers simultaneously into one high-finesse cavity, both the pumping efficiency and probing sensitivity are significantly enhanced. Foltynowicz *et al.*[35,36] recently used a comb to probe OODR absorption transitions of CH_4 and took advantage of the comb to cover a broad spectral range. Here, we present a full description of the

COCA-DR method and demonstrates all three types of double-resonance spectroscopy. We also give corrections due to the recoil effect and the second-order Doppler shift in precise OODR measurements. The V-type and Λ-type DR spectra of $^{12}C^{16}O$ are used to verify the accuracy of the transition frequencies obtained by the method. The ladder-type DR measurements determine the energy of a highly excited state of CO, which is compared to the previous Doppler-broadened cavity ring-down spectroscopy measurement of the single-photon transition from the ground state. We also discuss the uncertainty budget of the line positions obtained by this method and outlook for potential applications in various studies.

II. METHOD

Consider a molecule with rest mass M. By absorbing a photon with frequency ω in the lab system of reference, the molecule is pumped to the excited state and the molecular velocity changes from $\vec{v}_i$ to $\vec{v}_f$. The difference between the initial and final energy levels is $\hbar\omega_0$, where $\hbar$ is the Planck constant. Taking into account the relativistic energy conservation and the momentum conservation,[37] we have

$$\omega - \omega_0 = \vec{k}\cdot\vec{v}_i - \omega_0\frac{v_i^2}{2c^2} + \omega_0\frac{\hbar\omega_0}{2Mc^2} + \cdots, \tag{1}$$

where c is the speed of light and $\vec{k}$ is the wave vector of the photon in the lab system of reference ($k = \omega/c$). Terms on the right-hand side of Eq. (1) correspond the first-order Doppler shift, the second-order Doppler shift, and the recoil shift, respectively. Taking the CO transition at 1.56 μm as an example, the fractional correction due to the recoil effect is 1.5×10^{-11}. The relative second-order Doppler shift is 1×10^{-12} if we use the most probable speed of carbon monoxide at room temperature.

Taking the laser propagating direction as the z axis, the resonant condition is fulfilled only for molecules having an initial speed of v_{zi},

$$v_{zi} = c\left[1 - \frac{\omega_0}{\omega} + \frac{v_i^2}{2c^2} - \frac{\hbar\omega}{2Mc^2}\right]. \tag{2}$$

Since the second-order Doppler shift and recoil shift are relatively small, the difference between ω and ω_0 has been neglected in these two terms. Note that after absorption, molecules in the higher state have a different speed along the z-axis: $Mv_{zf} = Mv_{zi} + \hbar\omega/c$. Therefore, we have

$$v_{zf} = c\left[1 - \frac{\omega_0}{\omega} + \frac{v_i^2}{2c^2} + \frac{\hbar\omega}{2Mc^2}\right]. \tag{3}$$

Now, we consider a molecule interacting with two counter-propagating light beams. In the Λ-type double resonance, two transitions share the same upper state [see the green line shown in Fig. 1(a)], and we can derive the DR condition using Eq. (3),

$$\left[1 - \frac{\omega_{10}}{\omega_1} + \frac{v^2}{2c^2} + \frac{\hbar\omega_1}{2Mc^2}\right] = -\left[1 - \frac{\omega_{20}}{\omega_2} + \frac{v^2}{2c^2} + \frac{\hbar\omega_2}{2Mc^2}\right], \tag{4}$$

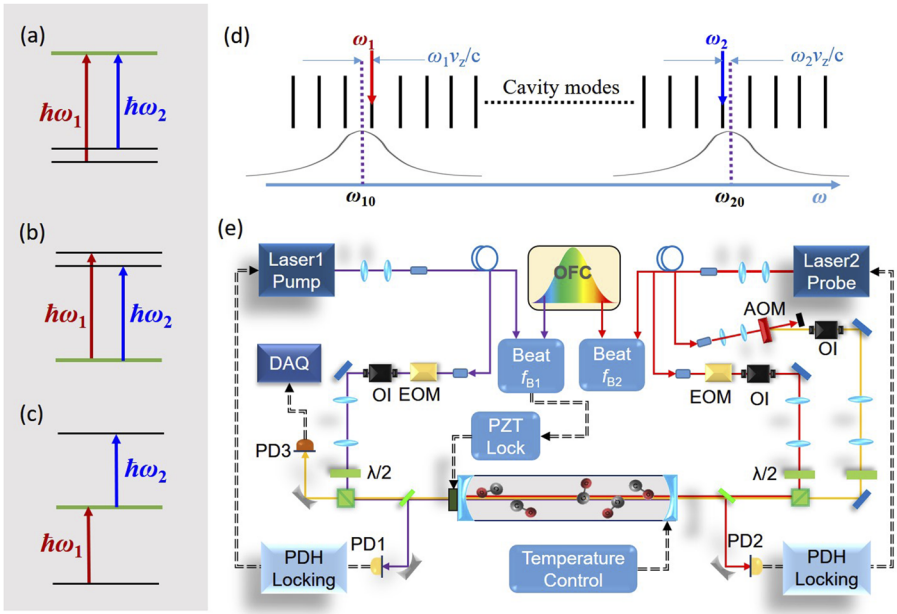

FIG. 1. Three different types of double resonances: (a) Λ-type, (b) V-type, and (c) ladder-type. (d) Principle of the comb-locked cavity-assisted double resonance (COCA-DR) method. Frequencies of two lasers are denoted as ω_1 and ω_2, which are locked on two cavity modes. These two lasers' frequencies are shifted from two molecular transition centers (ω_{10} and ω_{20}) by $\omega_1 v_z/c$ and $-\omega_2 v_z/c$, respectively. Here, c is the speed of light and v_z is the speed of molecule along the laser propagating direction. (e) Configuration of the COCA-DR experimental setup. Three laser beams, pumping, probe laser locking, and cavity ring-down spectroscopy (CRDS) probing, are shown in purple, red, and dark yellow colors, respectively. Abbreviations—AOM: acousto-optical modulator; DAQ: data acquisition card; EOM: electro-optical modulator; OFC: optical frequency comb; OI: optical isolator; PD: photodiode detector; and PZT: piezoelectric actuator.

$$\left(1-\frac{\omega_{10}}{\omega_1}\right)+\left(1-\frac{\omega_{20}}{\omega_2}\right)+\frac{v^2}{c^2}+\frac{\hbar(\omega_1+\omega_2)}{2Mc^2}=0. \quad (5)$$

Here, ω_{10} and ω_{20} are resonant frequencies of two molecular transitions and ω_1 and ω_2 are frequencies of two lasers. Note that the term of second-order Doppler shift is very relatively small, and we replace $v_i^2/2c^2$ with $v^2/2c^2$ for simplicity.

A V-type double resonance occurs when two transitions have the same lower state, and the condition [according to Eq. (2)] is

$$\left(1-\frac{\omega_{10}}{\omega_1}\right)+\left(1-\frac{\omega_{20}}{\omega_2}\right)+\frac{v^2}{c^2}-\frac{\hbar(\omega_1+\omega_2)}{2Mc^2}=0. \quad (6)$$

As in the "ladder"-type double resonance, the first laser pumps molecules to an intermediate state and the second laser drives them to a higher state, and we have

$$\left(1-\frac{\omega_{10}}{\omega_1}\right)+\left(1-\frac{\omega_{20}}{\omega_2}\right)+\frac{v^2}{c^2}+\frac{\hbar(\omega_1-\omega_2)}{2Mc^2}=0. \quad (7)$$

Note that contributions from the recoil shift are different for these three types of double resonances. In the ladder-type DR, the recoil shift almost cancels if the two transition frequencies are close. As a comparison, in conventional saturation spectroscopy (Lamb-dip measurement), the recoil effect leads to a doublet[38] instead of a shift.

The principle of the COCA-DR method is illustrated in Fig. 1(d). Two single-mode lasers are locked with two longitudinal modes of a high-finesse cavity, and their frequencies are ω_1 and ω_2. They are also in the vicinity of two molecular transitions with center frequencies of ω_{10} and ω_{20}, respectively. We can change the cavity length to shift frequencies of the cavity modes and both lasers. Double resonance happens when both lasers are resonant with molecules with a specific speed of v_z along counter-propagating lasers.

In principle, the DR condition with co-propagating pump and probe light beams could also be considered. The DR conditions could be easily derived in the similar way. For example, the Λ-type DR condition could be obtained by removing the negative sign after the equal sign in Eq. (4). We have conditions for all three types of DR with *co-propagating* beams,

$$\begin{aligned}
&\frac{\omega_{10}}{\omega_1}-\frac{\hbar\omega_1}{2Mc^2}=\frac{\omega_{20}}{\omega_2}-\frac{\hbar\omega_2}{2Mc^2} && \Lambda-type,\\
&\frac{\omega_{10}}{\omega_1}+\frac{\hbar\omega_1}{2Mc^2}=\frac{\omega_{20}}{\omega_2}+\frac{\hbar\omega_2}{2Mc^2} && V-type,\\
&\frac{\omega_{10}}{\omega_1}-\frac{\hbar\omega_1}{2Mc^2}=\frac{\omega_{20}}{\omega_2}+\frac{\hbar\omega_2}{2Mc^2} && ladder-type.
\end{aligned} \quad (8)$$

Therefore, two lasers must be both blue-shifted or both red-shifted. Note that all the cavity modes move in the same direction when the cavity length changes. We could find that it is hard to fulfill the DR conditions with co-propagating beams with both lasers near resonance with the molecule. In the case of the counter-propagating beams, as illustrated in Fig. 1(d), we are always able to fulfill the DR conditions [Eqs. (5)–(7)] with a small change in the cavity length, letting one laser *blue* shifted and the other laser *red* shifted. As ω_1 and ω_2 could be determined experimentally, one can determine the one of the molecular transition centers (ω_{10}, ω_{20}) if the other one is known.

III. EXPERIMENT SETUP

A schematic configuration of our experimental setup is given in Fig. 1(e). Two external-cavity diode lasers (Toptica DL100 Pro) were used. Both lasers were locked with respective modes of the optical cavity using the Pound–Drever–Hall (PDH) method.[39] Modulation frequencies for pump and probe laser PDH locking are 21 and 20 MHz, respectively. The optical cavity is composed of a pair of high-reflective (HR) mirrors (Layetec, radius of curvature ~1 m). The cylindrical spacer of the cavity is made of an Invar alloy and temperature-stabilized with a drift less than 10 mK. The distance between two HR mirrors is $L \approx 108$ cm, resulting in a free spectral range (FSR) of about 139 MHz. The laser beam waist has been aligned at the center of the cavity, and its radius is estimated to be 0.5 mm. The whole cavity is enclosed in a stainless-steel vacuum chamber, which can be pumped to 10^{-5} Pa by a turbo molecular pump.

In the DR measurement, one laser is noted as the "pump" and the other one is noted as the "probe." The probe laser is split into two beams: One is used to lock the laser frequency with a cavity mode, and the other one is used for cavity ring-down spectroscopy (CRDS)[40] measurements. The experimental method of CRDS is similar to that given in our previous study.[41,42] Three laser beams, pumping, probe laser locking, and CRDS probing, shown in different colors in Fig. 1(e), are aligned collinearly in the cavity. An acousto-optic modulator (AOM) is inserted in the CRDS probing beam. The driving radio frequency of the AOM is set precisely equal to the FSR of the cavity. Therefore, the CRDS probing beam can also pass through the cavity when the probe laser (locking beam) is locked with the cavity. The CRDS probing beam transmitted from the cavity is collected by a photodiode detector [PD3 in Fig. 1(e)]. A combination of Glan–Taylor calcite polarizers, waveplates, and polarized beam splitters (not all shown in Fig. 1) is used to separate the transmitted CRDS probing beam from other beams. Residual pumping and probe laser locking beams yield a relatively low and stable background and have negligible interference with the CRDS signal. The AOM driver is controlled by a rectangular wave with a frequency of about 500 Hz, resulting in the same repetition rate of the ring-down events. The CRDS decay time is derived by fitting the ring-down signal with an exponential decay function. The absorption coefficient of the sample inside the cavity is derived according to the equation $\alpha = (c\tau)^{-1} - (c\tau_0)^{-1}$, where τ and τ_0 are decay times with and without the sample, respectively. The decay time of the empty cavity was measured to be about 95 μs at 1.56 μm. The reflectivity of the HR mirror is determined to be $r = 0.999\,962$ according to the relation[43] $c\tau_0 = L/(1-r)$, indicating a cavity finesse of $F \approx 83\,000$. Consequently, the width of each cavity mode is FSR/$F \approx 1.6$ kHz. The transmittance of the cavity was measured to be 2.1% at 1.56 μm. According to the formula given in Refs. 44 and 45, the transmittance of the HR mirror is determined to be 6 ppm and the laser power (unidirectional) inside the cavity is enhanced to about 4000 times the input power. Note that the HR mirror reflectivity (cavity finesse as well) varies with the wavelength. At the wavelength of 1.64 μm, the ring-down time of the empty cavity increases to 158 μs ($r = 0.999\,977$) and the cavity transmittance becomes 6%.

Frequencies of the lasers are calibrated by an optical frequency comb. The comb is synthesized by an Er-fiber oscillator operated at 1.56 μm. Its repetition frequency ($f_R \approx 184$ MHz) and carrier offset

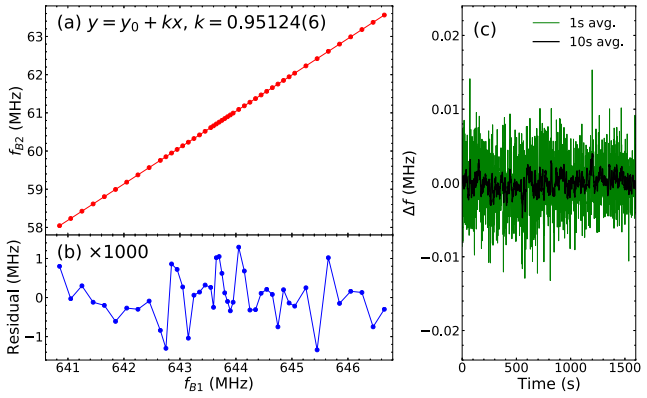

FIG. 2. (a) Tuning dependence between two laser frequencies both locked with the cavity. Laser 1 was tuned at 191.36 THz (1567 nm), and laser 2 was at 182.01 THz (1647 nm). Here, beat frequencies, f_{B1} and f_{B2}, are between two lasers and respective comb teeth. Each data point was obtained with an averaging time of 20 s. (b) Residuals (multiplied by a factor of 1000) of a linear fit of the laser frequencies. (c) Long-term drift of the probe laser frequency when f_{B1} was fixed.

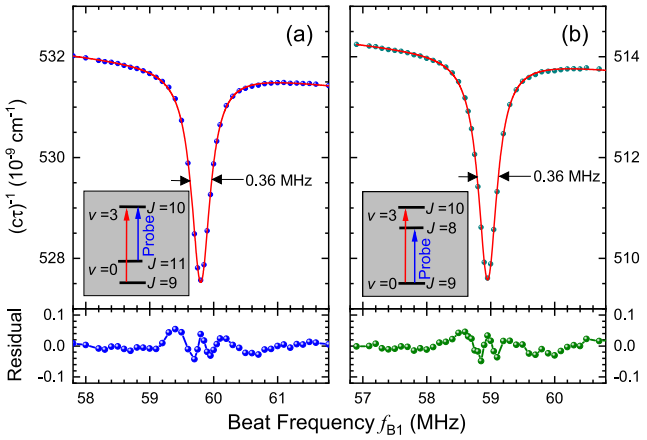

FIG. 3. COCA-DR spectra of (a) Λ-type and (b) V-type double resonance. Scattered points are experimental data, and the solid lines show those fitted with Lorentzian profiles. Spectra were averaged from about 60 scans recorded in about 1.5 h. Sample pressure: 0.7 Pa. Intracavity laser power: 14 W (pump) and 9 W (probe).

frequency ($f_0 \approx 20$ MHz) are referenced to a global position system (GPS)-disciplined rubidium clock (SRS FS725). Beat frequencies between both lasers and the frequency comb are registered (f_{B1} and f_{B2}). A feedback control servo was applied to a PZT attached to one of the HR mirrors, which changes the cavity length to lock the beat frequency f_{B1}. Consequently, the cavity length and both lasers are locked with the comb. By changing the frequency f_{B1} set in the PZT-locking servo, we can change the cavity length and perform simultaneous frequency tuning of both lasers. Figure 2(a) shows the linear dependence between f_{B2} and f_{B1}. Note that laser 1 was tuned at 1567 nm, laser 2 was tuned at 1647 nm, and the cavity was filled with sample gas in this measurement. As shown in Fig. 2(a), a linear fit gives a slope of 0.951 24(6), indicating a difference in tuning speeds of two lasers,[46] which needs to be considered in the frequency metrology. Figure 2(c) shows that the long-term drift of the laser frequency has been controlled well below a few kilohertz.

IV. RESULTS AND DISCUSSIONS

The COCA-DR method was tested by measuring overtone transitions of carbon monoxide. The CO sample was purified with the "freeze–pump–thaw" method before use, and the typical sample pressure was 0.7 Pa measured by a manometer (Pfeiffer CCR364), which has an accuracy of about 0.1 Pa. The sample cavity was temperature-stabilized at 298.6 K. Three different types of DR spectra were measured. In these measurements, the "pump" laser was tuned near 1566.6 nm, where locates the R(9) line in the (3 − 0) band of $^{12}C^{16}O$ (ν = 6383.0896 cm^{-1} and A = 0.007 46 s^{-1} from the HITRAN database[47]). The pump and probe laser powers were in the range of 2–4 mW before entering the cavity.

A. Λ- and V-type DR—accuracy and the uncertainty budget

Figure 3(a) shows the Λ-type DR spectrum recorded by tuning the probe laser frequency around 6302.40 cm^{-1}, close to the P(11) line in the same vibrational band. Here, the pump laser raised population in the upper state (V = 3, J = 10), and led to a dip in the probed transition sharing the same upper level. The V-type DR spectrum was recorded by tuning the probe laser close to the P(9) line in the same band (6312.07 cm^{-1}). Since the pump laser reduced the population in the common lower state (v = 0, J = 9), also a dip appears in the recorded spectrum, as shown in Fig. 3(b).

The sensitivity of the CRDS measurement, in terms of noise-equivalent absorption coefficient, was about 2×10^{-11} cm^{-1} after averaging about 60 spectra accumulated in 1.5 h. The noise level can also be seen from the fitting residuals shown in Fig. 3. The observed DR linewidth (full width at half maximum, FWHM) is 360 kHz at a sample pressure of 0.7 Pa. It mainly comes from transit-time broadening, which is estimated[44,48,49] to be 240 kHz with a beam waist of 0.5 mm and a temperature of 299 K. The lifetime of ro-vibrational levels of CO is at the millisecond level, and the natural linewidth is less than 1 kHz. The unidirectional laser power inside the cavity was estimated to be 14 W. Under our experimental conditions, the saturation parameter[50] is about 0.3 for the $R_{3-0}(9)$ line, leading to a power-broadening factor of 1.2. The CO transition has a pressure broadening coefficient of 0.128 cm^{-1} per atmosphere given in the HITRAN database,[47] corresponding to a linewidth (FWHM) of 27 kHz at 0.7 Pa. The observed linewidth is larger than the calculated value, and one possible reason is that the collision-induced broadening observed in Doppler-free spectroscopy measurements at low pressures (< 10 Pa) could be significantly larger than that derived from Doppler-broadened spectra.[51]

The DR spectra shown in Fig. 3 were fit by Lorentzian profiles, and the centers were obtained from the fit. Note that both laser frequencies were tuned simultaneously during the spectral scan. They were derived from the relationship between f_{B1} and f_{B2} (similar to that shown in Fig. 2) prior to the spectral scan under each experimental condition. Taking the frequency of the R(9) line determined from previous Lamb-dip measurements,[41] we used Eqs. (2)–(6) to

derive the velocity v_z and the frequency ω_{20}. The uncertainty of $\omega_{20}/2\pi$ is estimated to be 3.7 kHz, and the contributions are as follows:

(1) Statistical: As shown in Fig. 3, the maximum fitting residual is around 5×10^{-11} cm^{-1}, about 1/80 of the peak amplitude. Considering a DR spectral linewidth of about 0.4 MHz, we took 1/80 of the half linewidth, which is 2.5 kHz, as the uncertainty due to the limited signal-to-noise ratio, which is also consistent with the deviation among different runs of the measurement.

(2) Calibration: Frequencies of both lasers were derived from the beat signal with the frequency comb. The f_r frequency of the comb is controlled by the GPS-disciplined rubidium clock (SRS FS725), which has a fractional uncertainty of 2×10^{-12} at an averaging time of 100 s. It corresponds to an uncertainty of 0.4 kHz at 1.6 μm. Calibration uncertainties from other sources are negligible.

(3) Line profile: There is ambiguity in the baseline and line profile model applied in the fitting. The DR peak is actually on top of a Doppler-broadened absorption feature, which has a width of about 400 MHz. Another source of the non-flat baseline is the "fringe" coming from parasitic etalons in the optical path, which usually has a period of several hundred MHz or larger. Since the DR spectrum considered here only spreads in a range of a few MHz, we simply use a straight line as the baseline in the fit. The Lorentzian function was used to fit the DR peak, and Fig. 3 indicates that residuals near the peak center are about 2% of the peak height. The deviation could be reduced by using the Voigt profile in the fit, but the deviation around the peak center is still higher than that far from the center. The peak center derived from the fitting has no considerable difference by using different symmetric line profile models. However, any asymmetry in the profile would significantly change the "center" of the peak. Since the frequency of the pump laser is also changing during the spectral scanning process, the number of excited molecules will change monotonously within the scan range, which may be a source of line profile asymmetry. As shown in Figs. 3 and 4, the observed asymmetry in the fitting residuals is below 1% of the peak height. Therefore, we give an uncertainty of 2 kHz due to the line profile model, which is 1% of the half width of the peak.

(4) Collision-induced shift: Picqué and Guelachvili reported[52] self-induced pressure line shift coefficients of about -0.006 cm^{-1} atm^{-1} (-1.8 kHz/Pa) based on Doppler-broadened absorption spectroscopy of the (3 − 0) band of CO. However, we have not observed any pressure-dependent frequency shift within our experimental uncertainty in the range of 0.2–1 Pa. According to the previous Lamb-dip measurement,[41] we attribute an uncertainty of 0.2 kHz for the possible contribution from the pressure-related frequency shift.

(5) Power shift: Under our experimental conditions, spectra were taken with intra-cavity laser powers in the range of 5–20 W, corresponding to a saturation parameter[41,50] of about 0.2–0.7. We did not observe any frequency shift within the experimental uncertainty. As a conservative estimation, we give an uncertainty of 1 kHz, taking into account systematic shifts due to laser power-related effects under present experimental conditions.

(6) Others: Other contributions to the uncertainty budget, such as those from the laser wavefronts' curvature, high-order Doppler shift, AC Stark effect, and gas-lens effect,[53] are estimated to be well below 0.5 kHz. In particular, we did not observe any power-dependent shift within our experimental uncertainty. The uncertainty in ω_{10} also needs to be included in the determination of ω_{20}.

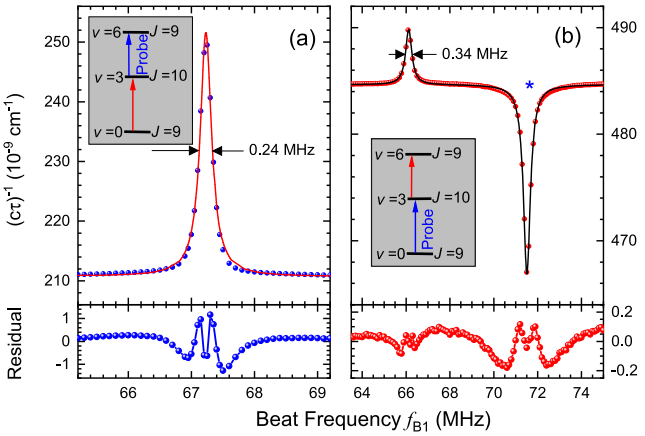

FIG. 4. COCA-DR spectra of the ladder-type double resonance. Scattered points are experimental data, and the solid lines show those fitted with Lorentzian profiles. (a) Probing near the $P_{6-3}(10)$ line. Sample pressure: 0.3 Pa. Intracavity laser power: 5 W (pump) and 16 W (probe). (b) Probing near the $R_{3-0}(9)$ line. Sample pressure: 0.7 Pa. Intracavity laser power: 12 W (pump) and 12 W (probe). The dip marked by "*" corresponds to the Lamb dip of the $R_{3-0}(9)$ transition, and the peak is from the COCA-DR signal.

The final results are given in Table I, together with the uncertainties discussed above. The ω_{20} values agree well with those

TABLE I. Transition frequencies (in kHz 2π) observed in Λ- and V-type DR spectra of CO. The values in parentheses are 1σ uncertainties in last digits.

ω_{10}[a]	$R_{3-0}(9)$: 191 360 212 764.0(0.5)	
	Λ type $R_{3-0}(9)$ and $P_{3-0}(11)$	V type $R_{3-0}(9)$ and $P_{3-0}(9)$
ω_1	191 360 187 252.0	191 360 244 301.7
ω_2	188 941 238 024.7	189 231 097 774.9
Recoil	5.7	−5.7
Second-order Doppler	0.4	0.4
v_z	−39.963(6) m/s	49.404(6) m/s
ω_{20}	188 941 212 841.3(3.7)	189 231 128 956.4(3.7)
ω_{20}[a]	188 941 212 844.5(1.0)	189 231 128 956.5(1.0)
Δ[b]	−3.2(3.8)	−0.1(3.8)

[a] Frequencies obtained from Lamb-dip measurements.[41,42]
[b] $\Delta = \omega_{20} - \omega_{20}$, where ω_{20} is the value derived from the DR measurement according to Eqs. (5) and (6).

obtained directly from Lamb-dip measurements.[41,42] The analysis above gives a consistency check of the accuracy of the DR measurement.

B. Ladder-type DR—detecting highly excited states

In the ladder-type DR measurements, the first laser (6383.09 cm^{-1}) excited the molecules to the intermediate state ($v = 3$, $J = 10$), and the second laser (6071.23 cm^{-1}) drove molecules from the intermediate state to the highly excited state ($v = 6$, $J = 9$). Figure 4(a) shows the absorption spectrum probed by the second laser. We have also switched lasers 1 and 2 in Fig. 1(e) without changing their wavelengths, leaving most of other optics unchanged. We probed the absorption signal of the first laser with the second laser kept on, and the spectrum is shown in Fig. 4(b). Note that the dip in Fig. 4(b) represents the Lamb dip of the line $R_{3-0}(9)$. The peak in Fig. 4(b) corresponds to the ladder-type DR signal. We can find that the spectrum shown in Fig. 4(a) has an excellent signal-to-noise ratio (~2000) and a flat background. The reasons are as follows: First, the transition dipole moment of the (6 − 3) band is larger than the (3 − 0) band, according to the calculated Einstein A coefficients of the transitions given by Li *et al.*[54] Second, only molecules whose speed fulfills the ladder-type DR condition [Eq. (7)] can be pumped to the intermediate state. Therefore, the baseline of the ladder-type DR spectrum is only the cavity loss. However, the Λ-type and the V-type DR peaks are on top of Doppler-broadened absorption profiles, as shown in Figs. 3(a) and 3(b). Note that the linewidth of the DR peak shown in Fig. 4(a) is narrower than others. A possible reason is that the spectrum was recorded at a relatively lower sample pressure (0.3 Pa), but more controlled measurements are needed before we can reach a conclusion. Moreover, fitting residuals around the line center shown in Fig. 4 are considerably larger than the noise level, indicating that the line profile actually deviates from the Lorentzian function applied in the fit. One reason could come from the CRDS measurement. The probe laser power changes during a ring-down event, while the double resonance signal is related to the laser power. Consequently, it leads to a deviation from the single exponential decay, which has not been considered in this work. The fitting residuals could be reduced by adding more tunable parameters in the line profile model, but more investigation is needed to understand the mechanism, which is beyond the scope of the present work and will be studied in the future.

The ladder-type DR spectrum shown in Fig. 4(a) allows us to determine the $P_{6-3}(10)$ line frequency precisely. We carried out measurements under different experimental conditions by selecting different cavity modes or changing the cavity temperature. Consequently, DR spectra of molecules with different speeds of v_z were recorded, and they are presented in Fig. 5(a). The v_z value was derived according to Eq. (3) for each spectrum. As the speed increases, the number density of probed molecules decreases and the observed DR peak amplitude decreases. Figure 5(b) shows the relative amplitudes of the DR peaks, which could be explained by the Boltzmann–Maxwell speed distribution of molecules at 299 K. For each measurement, the $P_{6-3}(10)$ line frequency (ω_{20}) was derived according to Eq. (7) and the results are illustrated in Fig. 5(c). Values of the frequency ω_{20} derived from spectra of different speeds agree well with each other, and we did not observe any speed dependence.

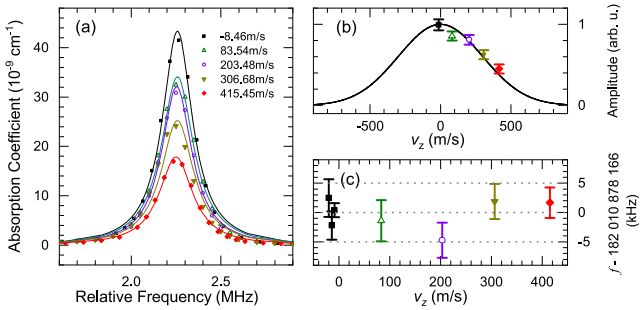

FIG. 5. (a) DR spectra of the $P_{6-3}(10)$ line observed by selecting molecules with different speeds along the laser beam (v_z): −8.46, 83.54, 203.48, 306.68, and 415.45 m/s. Sample pressure: 0.3 Pa. Intracavity laser power: 5 W (pump) and 15 W (probe). The first-order Doppler shift [see Eq. (1)] was added in each spectrum. (b) The scattered points are amplitudes of the observed DR peaks. The one close to the zero v_z speed is used to normalize other data. The solid line shows the Boltzmann speed distribution of CO molecules at 299 K. (c) Frequencies of the $P_{6-3}(10)$ line (ω_{20}) derived from COCA-DR measurements of CO molecules with different speeds (v_z) along the laser beam.

An average of the values yields $\omega_{P_{6-3}(10)}$ = 182 010 878.166(4) MHz 2π. As shown in Table II, taking the ground state rotation energy[55] and the $R_{3-0}(9)$ transition frequency, we derived the energy of the upper level ($v = 6$, $J = 9$) as 378 556 841.787(8) MHz $2\pi\hbar$. The energy has been determined to be 378 556 853(9) MHz $2\pi\hbar$ by a Doppler-limited CRDS measurement of the R(8) line in the (6 − 0) band of $^{12}C^{16}O$.[56] The value obtained in this work agrees with the previous result (1.3σ), and the accuracy has been improved by three orders of magnitude.

The double resonance measurement of the (6 − 0) overtone transition of CO is significantly more accurate than the previous Doppler-limited single-photon absorption spectroscopy measurement,[56] although both studies used the same cavity ring-down spectroscopy method. The reasons are as follows: First, as a Doppler-free measurement, the DR peak has a very narrow linewidth of a few hundred kilohertz, three orders of magnitude smaller than the Doppler width at room temperature. Second, in cavity-enhanced spectroscopy measurements, one can often see "fringes" rising from the parasitic étalon effect due to two reflecting surfaces in the optical path. When the period of the fringe is close to that of the spectral feature, it would be hard to separate the molecular spectrum

TABLE II. Energy of the ($v = 6$, $J = 9$) level of $^{12}C^{16}O$ (unit: MHz $2\pi\hbar$). Comparison between the value obtained in this work and that derived from the measurement of one-photon transition.[56]

	Frequency	Source
$E''_{v=0,J=8}$	4 148 838.472(8)	Reference 55
$R_{6-0}(8)$	374 408 015(9)	Reference 56
$E_{v=6,J=9}$	378 556 853(9)	Reference 56
$E''_{v=0,J=9}$	5 185 750.857(8)	Reference 55
$R_{3-0}(9)$	191 360 212.7640(5)	Reference 42
$P_{6-3}(10)$	182 010 878.166(4)	This work
$E_{v=6,J=9}$	378 556 841.787(9)	This work

from the fringe, and the line center derived from the spectrum could be shifted. Because lengths of parasitic étalons are usually in the range of several millimeters to tens of centimeters, corresponding to a frequency period of 10^2–10^4 MHz, the fringe effect is more serious in Doppler-limited single-photon absorption spectroscopy measurements. Since the DR measurement only needs to scan a frequency range of a few MHz, the fringe could be simply treated as a rather flat baseline. Moreover, in the ladder-type two-step DR measurement of vibrationally excited states, we probe the transition with less change in the vibrational quantum number than that in the one-step measurement. Consequently, the transition dipole moment in the DR measurement could be larger by a few orders of magnitude. For example, Einstein A coefficients of the $R_{3-0}(9)$ and $P_{6-3}(10)$ transitions have been calculated[54] to be 0.0075 and 0.13 s^{-1}, respectively. While the Einstein A coefficient of the $R_{6-0}(8)$ transition is only 1.1×10^{-7} s^{-1}. Because of the extremely small A coefficients, lines in the (6 − 0) overtone band could hardly be measured by saturation spectroscopy. Therefore, the COCA-DR method allows us to measure highly excited ro-vibrational energy levels of molecules with better accuracy and sensitivity.

V. CONCLUSION AND PERSPECTIVES

We have presented precise double resonance spectroscopy of molecules using continuous-wave diode lasers of milliwatts. The comb-locked cavity-assisted double-resonance (COCA-DR) method was established by locking two lasers to a high-finesse cavity and pumping molecules at a selected speed along the laser beam. Different recoil shifts are derived for all three types of double resonances in three-level systems. The method was demonstrated with infrared transitions of carbon monoxide. The observed DR spectra show a linewidth of a few hundred kHz, and the transition frequencies were determined with an accuracy of a few kHz. The accuracy is verified by comparing the results obtained from Λ- and V-type DR measurements and those from Lamb-dip studies. The energy of a rotation level in the highly excited $v = 6$ vibrational state was determined by the ladder-type DR measurement, with an accuracy one thousand times better than the previous result obtained from Doppler-limited absorption spectroscopy. It is also worth noting that the COCA-DR signal could be detected by methods other than absorption spectroscopy (CRDS in this work), such as the fluorescence measurement,[57,58] which could be more sensitive in some systems.

We have focused on the line positions and frequency accuracy in this work, and more information could be derived from the DR line intensities and profiles. For example, it allows for the determination of transition dipole moments among excited states, which could be compared with calculated values.[54] Relaxation and collision-induced effects might be investigated through the line profiles. The method could also be applied to label the transitions unambiguously. Combination differences are frequently used to assign ro-vibrational transitions of polyatomic molecules, but there are often wrong assignments due to accidental coincidence in a congested Doppler-limited spectrum. The COCA-DR method, in particular the V-type and the Λ-type, could be applied to check such combination differences directly. Doppler-free DR spectra have very narrow linewidths, which could effectively eliminate the possibility of accidental coincidence. It is also a welcome advantage in some challenging applications of optical trace analysis. An example is the optical (CRDS) detection of gaseous radiocarbon[59–61] using the mid-infrared transition of $^{14}CO_2$. One major challenge is to distinguish the $^{14}CO_2$ line from overlapping broad lines of other more abundant isotopes of CO_2 or contaminating molecules such as N_2O. The COCA-DR method has the potential to eliminate such interference without sacrificing the detection sensitivity if the pumping power is sufficiently high. We are currently developing[62] a prototype instrument of detecting $^{14}CO_2$ using the double-resonance spectroscopy method.

Miscellaneous pump–probe schemes of molecules interacting with multiple laser fields could be studied by the COCA-DR method. The resolving power of narrow-linewidth lasers used in the method allows for exploring the dynamics of molecular quantum states that could hardly be resolved before. The very high sensitivity allows for probing states that are hardly reached before. We have demonstrated measurements of molecules with selected quantum states and velocities, and we can foresee potential applications of the method in various studies, such as coherent population trapping, precision spectroscopy, trace analysis, and testing fundamental physics and symmetry.

ACKNOWLEDGMENTS

This work was jointly supported by the Chinese Academy of Science (Grant No. XDB21020100) and by the National Natural Science Foundation of China (Grant Nos. 21688102, 21427804, and 21903080).

DATA AVAILABILITY

The data that support the findings of this study are available from the corresponding author upon reasonable request.

REFERENCES

[1] H. R. Gray, R. M. Whitley, and C. R. Stroud, "Coherent trapping of atomic populations," Opt. Lett. **3**, 218 (1978).
[2] S. E. Harris, "Electromagnetically induced transparency," Phys. Today **50**, 36 (1997).
[3] M. Fleischhauer, A. Imamoglu, and J. P. Marangos, "Electromagnetically induced transparency: Optics in coherent media," Rev. Mod. Phys. **77**, 633 (2005).
[4] J. Vanier, "Atomic clocks based on coherent population trapping: A review," Appl. Phys. B **81**, 421 (2005).
[5] V. Shah and J. Kitching, "Advances in coherent population trapping for atomic clocks," in *Advances in Atomic, Molecular, and Optical Physics* (Elsevier Inc., 2010), Vol. 59, pp. 21–74.
[6] T. Hänsch, R. Keil, A. Schabert, C. Schmelzer, and P. Toschek, "Interaction of laser light waves by dynamic Stark splitting," Z. Phys. A: Hadrons Nucl. **226**, 293 (1969).
[7] R. Wynands and A. Nagel, "Precision spectroscopy with coherent dark states," Appl. Phys. B **68**, 1 (1999).
[8] C.-H. Zhang and G.-H. Sha, "Double resonance spectroscopy and molecular dynamics," Science **262**, 374 (1993).
[9] J. I. Steinfeld, I. Burak, D. G. Sutton, and A. V. Nowak, "Infrared double resonance in sulfur hexafluoride," J. Chem. Phys. **52**, 5421 (1970).
[10] R. G. Brewer, R. L. Shoemaker, and S. Stenhom, "Collision-induced optical double-resonance," Phys. Rev. Lett. **33**, 63 (1974).
[11] J. J. Hinchen and R. H. Hobbs, "Rotational relaxation studies of HF using ir double-resonance," J. Chem. Phys. **65**, 2732 (1976).

[12]D. J. Nesbitt and R. W. Field, "Vibrational energy flow in highly excited molecules: Role of intramolecular vibrational redistribution," J. Phys. Chem. **100**, 12735 (1996).
[13]A. Callegari, H. K. Srivastava, U. Merker, K. K. Lehmann, G. Scoles, and M. J. Davis, "Eigenstate resolved infrared–infrared double-resonance study of intramolecular vibrational relaxation in benzene: First overtone of the CH stretch," J. Chem. Phys. **106**, 432 (1997).
[14]T. Rickes, L. P. Yatsenko, S. Steuerwald, T. Halfmann, B. W. Shore, N. V. Vitanov, and K. Bergmann, "Efficient adiabatic population transfer by two-photon excitation assisted by a laser-induced Stark shift," J. Chem. Phys. **113**, 534 (2000).
[15]H. Y. Ling, H. Pu, and B. Seaman, "Creating a stable molecular condensate using a generalized Raman adiabatic passage scheme," Phys. Rev. Lett. **93**, 250403 (2004).
[16]M. E. Kaminsky, R. T. Hawkins, F. V. Kowalski, and A. L. Schawlow, "Identification of absorption lines by modulated lower-level population: Spectrum of Na_2," Phys. Rev. Lett. **36**, 671 (1976).
[17]R. Teets, R. Feinberg, T. W. Hänsch, and A. L. Schawlow, "Simplification of spectra by polarization labeling," Phys. Rev. Lett. **37**, 683 (1976).
[18]M. Siltanen, M. Metsälä, M. Vainio, and L. Halonen, "Experimental observation and analysis of the $3\nu_1(\Sigma_g)$ stretching vibrational state of acetylene using continuous-wave infrared stimulated emission," J. Chem. Phys. **139**, 054201 (2013).
[19]J. Karhu, J. Nauta, M. Vainio, M. Metsälä, S. Hoekstra, and L. Halonen, "Double resonant absorption measurement of acetylene symmetric vibrational states probed with cavity ring down spectroscopy," J. Chem. Phys. **144**, 244201 (2016).
[20]K. K. Lehmann, "Resonance enhanced two-photon cavity ring-down spectroscopy of vibrational overtone bands: A proposal," J. Chem. Phys. **151**, 144201 (2019).
[21]A. M. Lyyra, H. Wang, T.-J. Whang, W. C. Stwalley, and L. Li, "cw all-optical triple resonance spectroscopy," Phys. Rev. Lett. **66**, 2724 (1991).
[22]F. M. J. Cozijn, P. Dupré, E. J. Salumbides, K. S. E. Eikema, and W. Ubachs, "Sub-Doppler frequency metrology in HD for tests of fundamental physics," Phys. Rev. Lett. **120**, 153002 (2018).
[23]A Fast and S. A. Meek, "Sub-ppb measurement of a fundamental band rovibrational transition in HD," Phys. Rev. Lett. **125**, 023001 (2020).
[24]L.-G. Tao, A.-W. Liu, K. Pachucki, J. Komasa, Y. R. Sun, J. Wang, and S.-M. Hu, "Toward a determination of the proton–electron mass ratio from the Lamb-dip measurement of HD," Phys. Rev. Lett. **120**, 153001 (2018).
[25]S. Patra, M. Germann, J.-P. Karr, M. Haidar, L. Hilico, V. I. Korobov, F. M. J. Cozijn, K. S. E. Eikema, W. Ubachs, and J. C. J. Koelemeij, "Proton–electron mass ratio from laser spectroscopy of HD^+ at the part-per-trillion level," Science **369**, 1238 (2020).
[26]S. Albert, F. Arn, I. Bolotova, Z. Chen, C. Fábri, G. Grassi, P. Lerch, M. Quack, G. Seyfang, A. Wokaun, and D. Zindel, "Synchrotron-based highest resolution terahertz spectroscopy of the ν_{24} band system of 1,2-dithiine ($C_4H_4S_2$): A candidate for measuring the parity violating energy difference between enantiomers of chiral molecules," J. Phys. Chem. Lett. **7**, 3847 (2016).
[27]M. S. Safronova, D. Budker, D. DeMille, D. F. J. Kimball, A. Derevianko, and C. W. Clark, "Search for new physics with atoms and molecules," Rev. Mod. Phys. **90**, 025008 (2018).
[28]J. Karhu, K. Lehmann, M. Vainio, M. Metsälä, and L. Halonen, "Step-modulated decay cavity ring-down detection for double resonance spectroscopy," Opt. Express **26**, 29086 (2018).
[29]H. K. Srivastava, A. Conjusteau, H. Mabuchi, A. Callegari, K. K. Lehmann, G. Scoles, M. L. Silva, and R. W. Field, "Rovibrational spectroscopy of the v = 6 manifold in $^{12}C_2H_2$ and $^{13}C_2H_2$," J. Chem. Phys. **113**, 7376 (2000).
[30]W. K. Bischel, P. J. Kelly, and C. K. Rhodes, "Observation of Doppler-free two-photon absorption in the ν_3 bands of CH_3F," Phys. Rev. Lett. **34**, 300 (1975).
[31]W. H. Weber and R. W. Terhune, "Sub-Doppler double-resonance spectroscopy of NH_3 using a tunable-diode laser and a CO laser," Opt. Lett. **6**, 455 (1981).
[32]J. Karhu, M. Vainio, M. Metsälä, and L. Halonen, "Frequency comb assisted two-photon vibrational spectroscopy," Opt. Express **25**, 4688 (2017).
[33]G. Zhao, D. M. Bailey, A. J. Fleisher, J. T. Hodges, and K. K. Lehmann, "Doppler-free two-photon cavity ring-down spectroscopy of a nitrous oxide (N_2O) vibrational overtone transition," Phys. Rev. A **101**, 062509 (2020).
[34]C.-L. Hu, V. I. Perevalov, C.-F. Cheng, T.-P. Hua, A.-w. Liu, Y. R. Sun, Y. Tan, J. Wang, and S.-M. Hu, "Optical–optical double-resonance absorption spectroscopy of molecules with kilohertz accuracy," J. Phys. Chem. Lett. **11**, 7843 (2020).
[35]A. Foltynowicz, L. Rutkowski, I. Silander, A. C. Johansson, V. Silva de Oliveira, O. Axner, G. Soboń, T. Martynkien, P. Mergo, and K. K. Lehmann, "Sub-Doppler double-resonance spectroscopy of methane using a frequency comb probe," Phys. Rev. Lett. **126**, 063001 (2021).
[36]A. Foltynowicz, L. Rutkowski, I. Silander, A. C. Johansson, V. Silva de Oliveira, O. Axner, G. Soboń, T. Martynkien, P. Mergo, and K. K. Lehmann, "Measurement and assignment of double-resonance transitions to the 8900–9100 cm^{-1} levels of methane," Phys. Rev. A **103**, 022810 (2021).
[37]W. Demtröder, *Laser Spectroscopy: Basic Concepts and Instrumentation*, 3rd ed. (Springer, 2008), pp. 768–769.
[38]J. L. Hall, C. J. Bordé, and K. Uehara, "Direct optical resolution of the recoil effect using saturated absorption spectroscopy," Phys. Rev. Lett. **37**, 1339 (1976).
[39]R. W. P. Drever, J. L. Hall, F. V. Kowalski, J. Hough, G. M. Ford, A. J. Munley, and H. Ward, "Laser phase and frequency stabilization using an optical-resonator," Appl. Phys. B **31**, 97 (1983).
[40]A. Okeefe and D. A. G. Deacon, "Cavity ring-down optical spectrometer for absorption-measurements using pulsed laser sources," Rev. Sci. Instrum. **59**, 2544 (1988).
[41]J. Wang, Y. R. Sun, L.-G. Tao, A.-W. Liu, and S.-M. Hu, "Communication: Molecular near-infrared transitions determined with sub-kHz accuracy," J. Chem. Phys. **147**, 091103 (2017).
[42]J. Wang, Y. R. Sun, L. G. Tao, A. W. Liu, and S. M. Hu, "Erratum: 'Communication: Molecular near-infrared transitions determined with sub-kHz accuracy' [J. Chem. Phys. 147, 091103 (2017)]," J. Chem. Phys. **148**, 029902 (2018).
[43]P. Zalicki and R. N. Zare, "Cavity ring-down spectroscopy for quantitative absorption measurements," J. Chem. Phys. **102**, 2708 (1995).
[44]L.-S. Ma, J. Ye, P. Dubé, and J. L. Hall, "Ultrasensitive frequency-modulation spectroscopy enhanced by a high-finesse optical cavity: Theory and application to overtone transitions of C_2H_2 and C_2HD," J. Opt. Soc. Am. B **16**, 2255 (1999).
[45]J. Wang, Y. R. Sun, L.-G. Tao, A.-W. Liu, T.-P. Hua, F. Meng, and S.-M. Hu, "Comb-locked cavity ring-down saturation spectroscopy," Rev. Sci. Instrum. **88**, 043108 (2017).
[46]P. Bohlouli-Zanjani, K. Afrousheh, and J. D. D. Martin, "Optical transfer cavity stabilization using current-modulated injection-locked diode lasers," Rev. Sci. Instrum. **77**, 093105 (2006).
[47]I. E. Gordon, L. S. Rothman, C. Hill, R. V. Kochanov, Y. Tan, P. F. Bernath, M. Birk, V. Boudon, A. Campargue, K. V. Chance, B. J. Drouin, J.-M. Flaud, R. R. Gamache, J. T. Hodges, D. Jacquemart, V. I. Perevalov, A. Perrin, K. P. Shine, M.-A. H. Smith, J. Tennyson, G. C. Toon, H. Tran, V. G. Tyuterev, A. Barbe, A. G. Császár, V. M. Devi, T. Furtenbacher, J. J. Harrison, J.-M. Hartmann, A. Jolly, T. J. Johnson, T. Karman, I. Kleiner, A. A. Kyuberis, J. Loos, O. M. Lyulin, S. T. Massie, S. N. Mikhailenko, N. Moazzen-Ahmadi, H. S. P. Müller, O. V. Naumenko, A. V. Nikitin, O. L. Polyansky, M. Rey, M. Rotger, S. W. Sharpe, K. Sung, E. Starikova, S. A. Tashkun, J. V. Auwera, G. Wagner, J. Wilzewski, P. Wcisło, S. Yu, and E. J. Zak, "The HITRAN2016 molecular spectroscopic database," J. Quant. Spectrosc. Radiat. Transfer **203**, 3 (2017).
[48]C. J. Bordé, J. L. Hall, C. V. Kunasz, and D. G. Hummer, "Saturated absorption-line shape: Calculation of transit-time broadening by a perturbation approach," Phys. Rev. A **14**, 236 (1976).
[49]P. Dupré, "Dipole saturated absorption modeling in gas phase: Dealing with a Gaussian beam," J. Quant. Spectrosc. Radiat. Transfer **205**, 196 (2018).
[50]G. Giusfredi, S. Bartalini, S. Borri, P. Cancio, I. Galli, D. Mazzotti, and P. De Natale, "Saturated-absorption cavity ring-down spectroscopy," Phys. Rev. Lett. **104**, 110801 (2010).
[51]S. Twagirayezu, G. E. Hall, and T. J. Sears, "Frequency measurements and self-broadening of sub-Doppler transitions in the $\nu_1 + \nu_3$ band of C_2H_2," J. Chem. Phys. **149**, 154308 (2018).

[52]N. Picqué and G. Guelachvili, "Absolute wavenumbers and self-induced pressure lineshift coefficients for the 3 − 0 vibration–rotation band of $^{12}C^{16}O$," J. Mol. Spectrosc. **185**, 244 (1997).
[53]P. Cérez and R. Felder, "Gas-lens effect and cavity design of some frequency-stabilized He–Ne lasers," Appl. Opt. **22**, 1251 (1983).
[54]G. Li, I. E. Gordon, L. S. Rothman, Y. Tan, S.-M. Hu, S. Kassi, A. Campargue, and E. S. Medvedev, "Rovibrational line lists for nine isotopologues of the CO molecule in the $X^1\Sigma^+$ ground electronic state," Astrophys. J., Suppl. Ser. **216**, 15 (2015).
[55]G. Winnewisser, S. P. Belov, T. Klaus, and R. Schieder, "Sub-Doppler measurements on the rotational transitions of carbon monoxide," J. Mol. Spectrosc. **184**, 468 (1997).
[56]Y. Tan, J. Wang, X.-Q. Zhao, A.-W. Liu, and S.-M. Hu, "Cavity ring-down spectroscopy of the fifth overtone of CO," J. Quant. Spectrosc. Radiat. Transfer **187**, 274 (2017).
[57]J. J. L. Spaanjaars, J. J. ter Meulen, and G. Meijer, "Relative predissociation rates of OH ($A^2\Sigma^+$, $v' = 3$) from combined cavity ring down—Laser-induced fluorescence measurements," J. Chem. Phys. **107**, 2242 (1997).
[58]J. Luque, P. A. Berg, J. B. Jeffries, G. P. Smith, D. R. Crosley, and J. J. Scherer, "Cavity ring-down absorption and laser-induced fluorescence for quantitative measurements of CH radicals in low-pressure flames," Appl. Phys. B **78**, 93 (2004).
[59]I. Galli, S. Bartalini, S. Borri, P. Cancio, D. Mazzotti, P. De Natale, and G. Giusfredi, "Molecular gas sensing below parts per trillion: Radiocarbon-dioxide optical detection," Phys. Rev. Lett. **107**, 270802 (2011).
[60]A. J. Fleisher, D. A. Long, Q. Liu, L. Gameson, and J. T. Hodges, "Optical measurement of radiocarbon below unity fraction modern by linear absorption spectroscopy," J. Phys. Chem. Lett. **8**, 4550 (2017).
[61]G. Genoud, J. Lehmuskoski, S. Bell, V. Palonen, M. Oinonen, M.-L. Koskinen-Soivi, and M. Reinikainen, "Laser spectroscopy for monitoring of radiocarbon in atmospheric samples," Anal. Chem. **91**, 12315 (2019).
[62]Y.-D. Tan, C.-F. Cheng, D. Sheng, and S.-M. Hu, "Detection of radiocarbon dioxide with double-resonance absorption spectroscopy," Chin. J. Chem. Phys. (published online 2021).